Food and Bioprocess Technology
https://doi.org/10.1007/s11947-025-04030-1

RESEARCH

Soft-Shell Prawns (*Penaeus monodon*) Can Be Identified Using Hyperspectral Imaging and Machine Learning – A Novel Approach to Ensure Consistency, Accuracy and Speed

Iman Tahmasbian[1,2] · Negar Omidvar[2] · Tony Charles[3] · Shahla Hosseini Bai[2]

Received: 2 June 2025 / Accepted: 25 August 2025

Abstract
Soft-shell prawns (shrimps), which yield lower market value than their hard-shell counterparts, are currently identified through manual inspection—a subjective and inconsistent process. This study explores the use of shortwave infrared (SWIR; 950–2515 nm) hyperspectral imaging (HSI) combined with machine learning as a real-time, non-destructive alternative for classifying prawn shell hardness. A total of 380 farmed prawns spanning four manually assessed hardness categories were scanned using a HSI camera. Two classification models—support vector machine (SVM) and partial least squares discriminant analysis (PLS-DA)—were trained on 50% of the total samples (training data set) to associate spectral signatures with shell hardness classes and evaluated using the remaining 50% (independent test data set). PLS-DA marginally outperformed SVM in overall classification accuracy, achieving 92.1%, compared to SVM's 90% on the independent test set. Although SVM showed better performance for intermediate hardness classes, its higher misclassification rate for the extreme classes (hard and soft) made it slightly less reliable for practical application. Reduced sensitivity in the intermediate classes across both models likely stems from limited sample size and subjectivity in the manual reference classifications. These results demonstrate the potential of HSI as a consistent and objective tool for prawn classification, offering significant advantages for automating shell hardness assessment and sorting. Implementing this technology could enhance processing efficiency and product quality within the prawn industry.

Keywords Automated seafood sorting · Food quality assurance technology · Machine learning classification · Shrimp post-harvest assessment · Smart food inspection · Soft-shell prawn detection

Introduction

Soft-shell prawns, also known as shrimps, often resulting from soft shell syndrome or moulting, are typically considered low quality and command low market prices (Chong, 2022). Rigorous quality control and screening are essential to ensure prawns are sorted into batches of consistent quality, maintaining market value and purchaser confidence. Current practices heavily depend on manual sorting, where skilled workers visually inspect and separate soft-shell prawns based on shell texture and softness. This process is labour-intensive, subjective and prone to inconsistencies (Tahmasbian et al., 2024). Some studies have investigated the use of machine vision for monitoring the visual quality of prawns. For example, machine vision has been used for grading prawns based on shape, size and weight (Balaban et al., 1995; Lee et al., 2012; Luzuriaga et al., 1997; Pan et al., 2009; zhang et al., 2014). While some studies also investigated the use of conventional or greyscale images combined with machine and deep learning algorithms for detecting soft-shell prawns (Liu, 2020; Liu et al., 2016), the visual similarities between soft and hard-shelled individuals limit the effectiveness of these methods. Methods using conventional images often require computationally intensive image processing and data analysis techniques to detect visual differences, if any, among the prawns, and minor visual variabilities may still affect

✉ Iman Tahmasbian
iman.tahmasbian@dpi.qld.gov.au

[1] Department of Primary Industries, Queensland Government, Toowoomba, QLD 4350, Australia

[2] School of Environment and Science, Griffith University, Nathan, Brisbane, QLD 4111, Australia

[3] Australian Prawn Farms Pty Ltd, Ilbilbie, QLD 4738, Australia

Published online: 23 September 2025

prediction accuracy. As a result, advanced imaging technologies that provide information beyond the visual properties may offer a solution to this issue.

Hyperspectral imaging (HSI) is a real-time, non-destructive method that uses spectral reflectance to assess the physical and biochemical properties of samples based on their spectral signatures (Menesatti et al., 2010; Sun, 2010). HSI combines near-infrared spectroscopy (NIRS) with imaging, leveraging the chemical sensitivity of NIRS and the spatial resolution of imaging to enable non-destructive, high-throughput analysis of complex biological samples (Manley, 2014). The principles of HSI are rooted in vibrational spectroscopy, where absorption bands in the spectra of chemical compounds correspond to molecular vibrations. The large number of contiguous spectral bands acquired through HSI produces high-dimensional datasets, which are often difficult to interpret directly. To address this, chemometrics—applying multivariate statistical and machine learning methods to chemical data—is commonly employed to analyse the data and develop predictive classification models (Park & Lu, 2015; Siesler et al., 2008). HSI combined with chemometrics has been used to monitor the internal quality attributes of prawns. Applications include monitoring changes in chemical composition (Xi et al., 2025) moisture and elasticity during hot air drying (Xu et al., 2022), assessing freshness (Qu et al., 2015; Ye et al., 2020), monitoring shelf-life (Siripatrawan & Makino, 2025), detecting environmental origin (Sun et al., 2019) and evaluating the mechanical properties of peeled prawns (Dai et al., 2014). However, the application of HSI to identify soft-shell prawns has not yet been investigated.

According to Beer's law, the amount of light absorbed or reflected by a substance at a particular wavelength is determined by its absorptivity or reflectivity, the length of the optical path and the substance's concentration (Siesler et al., 2008). In prawns, soft- and hard-shell individuals differ in mineral composition, concentration and shell thickness (Baticados et al., 1986, 1987; Li & Cheng, 2012; Vijayan & Diwan, 1996), factors that influence the parameters of Beer's law. Therefore, we hypothesised that variations in shell properties would affect the prawns' spectral signatures, enabling differentiation between shell hardness levels. This study aimed to investigate the potential of HSI combined with machine learning for classifying prawns according to their shell hardness, enabling the accurate and consistent identification of soft-shelled individuals, with potential integration into automated sorting systems.

Materials and Methods

Samples

The prawn samples used in this experiment were commercially farmed tiger prawns *(Penaeus monodon)*. The prawns were sourced from Australian Prawn Farms Pty Ltd., located in Ilbilbie, Queensland, Australia, a region characterised by a subtropical climate.

A total of 380 prawn samples were harvested in May 2023 from the same pond, where water quality remained constant (salinity = 31 to 32.5 ppt, pH = 7.2 to 7.6), and temperature was 25 °C. The only known variables between the samples were the level of shell hardness, including soft, just failed (JF), just passed (JP) and hard, and prawn sizes (small, medium, large and extra-large). Commercially, JF prawns would still be classified as soft in manual sorting, while JP prawns would be classified as hard. Due to practical limitations, achieving a fully balanced dataset in terms of sample numbers across classes was not feasible; however, the two main classes—soft and hard—were nearly balanced (Table 1).

The hardness level of the prawns was manually determined by skilled workers through tactile inspection, a standard practice on prawn farms. The manual classification was carried out immediately after harvest. The prawn samples were then placed in resealable plastic bags, stored in a cool box with ice and shipped overnight to the HSI laboratory. Upon arrival, the samples were promptly scanned using a HSI camera.

Hyperspectral Image Acquisition

The HSI system used in this study was a shortwave infrared (SWIR) system, consisting of a 16-bit line scan SWIR camera (HySpex, SWIR-384, Norsk Elektro Optikk, Oslo, Norway) operating in the spectral range of 950–2515 nm, with spectral sampling intervals of 5.45 nm. The SWIR system included two linear DC halogen lights (100 W each) positioned at a 45° angle to illuminate the camera's field of view, a translating stage and the Breeze software (version 2022.1.0; Umeå, Prediktera, Sweden). The setup of the SWIR HSI system is depicted in Fig. 1.

The prawn samples were placed on a black foam platform on the translating stage of the camera and scanned (Fig. 1). A dark image was captured before and after each

Table 1 Prawn sample numbers of different harness and size classes used in this study

	Small	Medium	Large	Extra-large	Total
Hard	58	48	28	32	166
JP	0	36	0	0	36
JF	6	14	16	0	36
Soft	48	36	32	26	142

Small: 68–88 prawns per kg; medium: 46–66 prawns per kg; large: 35–44 prawns per kg; extra-large: 22–33 prawns per kg

JP just passed,,*JF* just failed.

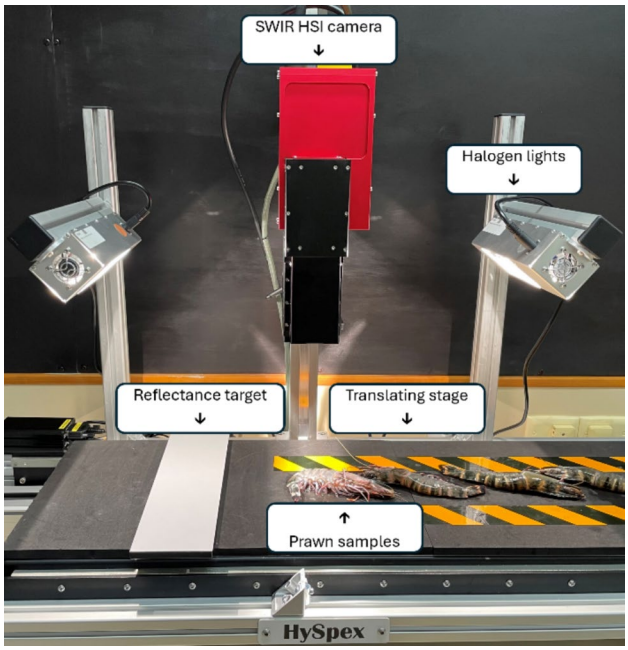

Fig. 1 The shortwave infrared (SWIR, 950–2515 nm) HSI system used for scanning prawns in the current study

scan to measure and correct for sensor errors (Seididamyeh et al., 2024). A Zenith standard reflectance board with 50% reflectance was scanned before each sample to convert raw data into reflectance values and calibrate for light variations during the experiment. This process, known as image correction (dark and white correction), was performed using (1):

$$R\ (\%) = \frac{R_0 - D}{W - D} \times RT \tag{1}$$

where R represented the corrected reflectance image; R_0 was the raw spectral image; D was the dark reference image; W was the white target image; RT was the reflectance percentage of the standard target.

Data Preparation

Background pixels were identified and removed based on reflectance thresholds at 1515 nm < 1.4% and 1951 nm < 2%, with these wavelengths selected through visual observation. The remaining sample images were cropped into smaller sections, each containing a single prawn. The prawn images, representing various sizes and hardness levels, were randomly split into the calibration and independent testing groups, each comprising 50% of the samples. Data transformation, including Savitzky–Golay smoothing filter, standard normal variate (SNV) and the first derivative was used individually and combined for increasing the signal to noise ratio and improve the accuracy (Gama et al., 2024). The calibration images were used to train models by correlating their spectral data with the pre-determined hardness levels, ensuring each class included samples from all available size categories.

Classification Modelling

We developed and compared two classification models including support vector machine (SVM) and partial least square discriminant analysis (PLS-DA). SVM and PLS-DA are among the best performing and widely used classifiers for spectral data in food science (Lu et al., 2025; Seididamyeh et al., 2024; Siripatrawan & Makino, 2024; Tahmasbian et al., 2021; zhang et al., 2016).

An optimised-SVM classification model with different kernel functions was trained using the calibration data set. The Bayesian optimisation method was used with a K-fold cross-validation ($K = 10$) to optimise the model parameters and improve the model's accuracy. The kernel functions included Gaussian, linear, quadratic and cubic. The process was repeated with transformed data. The SVM models were developed using Statistics and Machine Learning Toolbox for MATLAB (version R 2021a; The Math Works, Natick, USA).

The PLS-DA classification model was also trained using the same calibration data set. The PLS-DA model was optimised based on the coefficient of determination (R^2) in the cross-validation ($K = 10$) set by selecting the latent variable (LV) that produced the highest R^2. The PLS-DA classification modelling was conducted using Breeze software (version 2022.1.0; Umeå, Prediktera, Sweden).

Evaluation

The classification models' performance was assessed on the independent test data set using a confusion matrix and the statistical metrics defined in (2) to (6).

$$\text{Classification accuracy}(\%) = \frac{TP + TN}{TP + FP + TN + FN} \times 100 \tag{2}$$

$$\text{Sensitivity}\ (\%) = \frac{TP}{TP + FN} \times 100 \tag{3}$$

$$\text{Specificity}\ (\%) = \frac{TN}{TN + FP} \times 100 \tag{4}$$

$$\text{Precision}\ (\%) = \frac{TP}{TP + FP} \times 100 \tag{5}$$

$$\text{F1 score} = 2 \times \frac{Precision \times Sensitivity}{Precision + Sensitivity} \quad (6)$$

where *TP* is true positive; *TN* is true negative; *FP* is false positive; and *FN* is false negative. The F1 score ranges from 0 to 1, with values closer to 1 indicating better classification performance (Chicco & Jurman, 2020).

Results

Spectral Features

The spectral signatures of prawns with different shell hardness levels were relatively similar; however, the differences between the hardness classes were distinguishable across multiple wavelengths (Fig. 2). Three major spectral regions were identified, where significant deviations between the hardness classes occurred: 950–1130 nm (Region 1), 1163–1310 nm (Region 2) and 2204–2515 nm (Region 3) (Fig. 2). The difference between the shell hardness classes was more pronounced in Region 1, where a downward peak occurred at 989 nm, followed by an upward peak at 1059 nm (Fig. 2). Slightly smaller differences were observed in Region 2, where the second downward and upward peaks occurred at 1207 nm and 1277 nm, respectively. In Region 3, the differences between the reflectance of the hardness classes were less pronounced than in Regions 1 and 2. However, a shift in the spectral signatures was noted in this region, with soft-shell prawns reflecting less than hard-shell prawns. While this shift occurred at 1387 nm, the distinction between soft- and hard-shell prawns was more noticeable within Region 3.

The average spectral signatures of the JP and JF classes did not fall between those of the soft and hard classes. The average spectral signature of the JF class was consistently lower than that of the other three classes. The JP class, however, generally positioned between the soft and hard classes, with the exception of Region 1 (Fig. 2).

Classification Properties

The best performance of the optimised SVM classification model was achieved with the linear kernel function and SNV transformed data. The SVM parameters were selected at the lowest observed classification error (Fig. 3a). Classification accuracy of the SVM in the calibration and test sets were 92.30% and 90.00%, respectively.

The SVM model achieved 94.74% accuracy in classifying hard-shell prawns, with 2.44% misclassified as

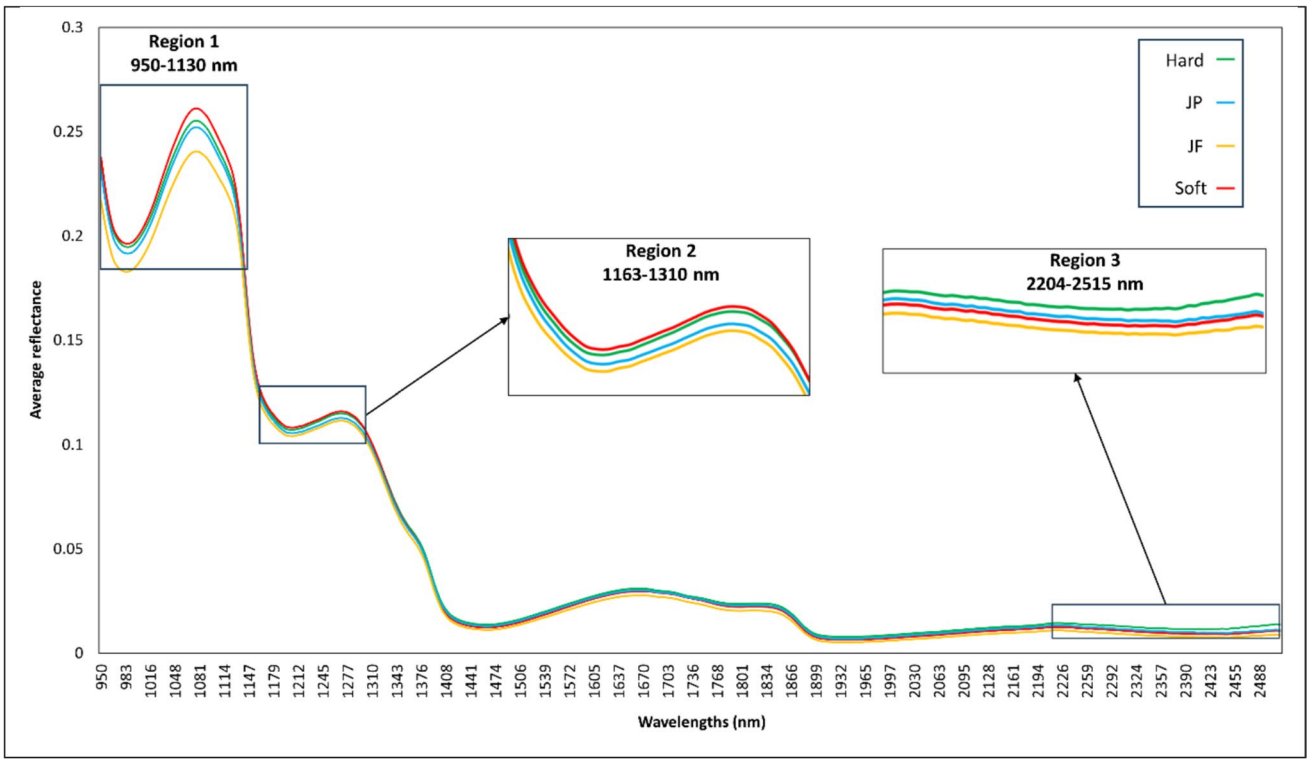

Fig. 2 Average reflectance (spectral signature) of the prawns with different shell hardness levels quantified in the shortwave infrared (950–2500 nm). The Regions 1–3 show the areas, where the differences between the soft- and hard-shell prawns were considerable. JP represents just passed, and JF represents just failed classes

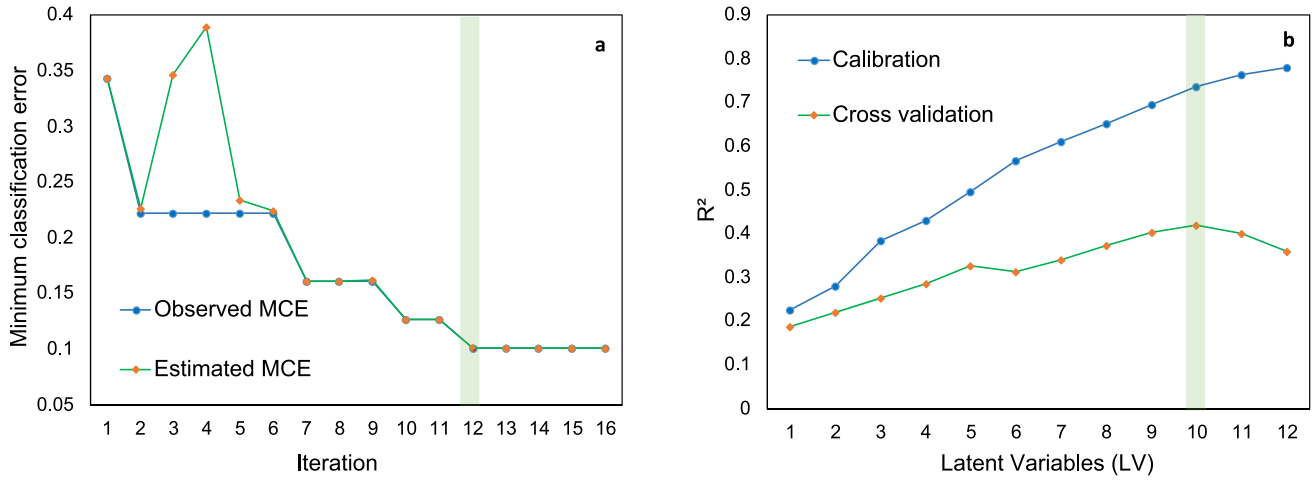

Fig. 3 Parameter optimisation of **a** support vector machine (SVM) and **b** partial least squares discriminant analysis (PLS-DA) using Bayesian optimisation and coefficient of determination (R^2) in the cross-validation dataset, respectively. The SVM parameters and PLS-DA latent variables (*LV*) were selected at the minimum classification error (*MCE*) and highest R^2, respectively

either JP or soft (Table 2.). The classification accuracy for soft-shell prawns was lower at 92.11%, with 8.33% of these prawns misclassified as hard, indicating confusion between the extreme classes. The highest misclassification rate was observed in the JF class, where 27.78% of samples were incorrectly classified as either soft or hard, resulting in a class accuracy of 95.26%. This was followed by the JP class, where 11.11% of samples were misclassified as JF or soft, resulting in a class accuracy of 97.89%. Notably, no samples remained unclassified when using the SVM model (Table 2.).

The PLS-DA model achieved optimal performance at 10 latent variables (*LV*s) (Fig. 3b). The classification accuracy was 94.21% for the calibration dataset and 92.10% for the independent test dataset (Table 2.). The summary of the model performance in classifying the prawn samples in the independent test dataset is presented in Table 2..

In general, the PLS-DA model outperformed the SVM, achieving 2.10% higher overall classification accuracy (Table 2.). The PLS-DA model correctly classified 97.37% of the soft-shell prawns and 99.47% of the hard-shell prawns. The sensitivity of the PLS-DA model was

Table 2 Confusion matrix of prawn classifications by the support vector machine (SVM) and the partial least square discriminant analysis (PLS-DA) model versus actual classes in the test set, with performance metrics for shell hardness classification

		Total	SVM					PLS-DA				
			Hard	JP	JF	Soft	UC	Hard	JP	JF	Soft	UC
Actual classes	Hard	82	**80**	1	-	1	-	**82**	-	-	-	-
	JP	18	-	**16**	1	1	-	-	**16**	-	-	2
	JF	18	2	-	**13**	3	-	1	-	**9**	1	7
	Soft	72	6	1	3	**62**	-	-	-	-	**68**	4
	Precision		90.91	88.89	76.47	92.54		98.80	100	100	98.60	
	Sensitivity		97.56	88.89	72.22	86.11		100	88.90	50	94.40	
	Specificity		92.59	98.84	97.67	95.76		99.10	100	100	99.20	
	F1 score		94.12	86.67	78.05	89.21		99.39	94.12	66.67	96.45	
	Class accuracy		94.74	97.89	95.26	92.11		99.47	98.95	95.26	97.37	
	Overall accuracy		90.00					92.10				

Accuracy, precision, sensitivity and specificity are expressed as percentages (%). Bolded values indicate the number of correctly classified samples for each class

JP just passed, *JF* just failed, *UC* unclassified

significantly lower than that of SVM in the intermediate class of JF (50% vs. 72.22%). Unclassified samples had the largest contribution to the low sensitivity (true positive rate) of the JF class, with 38.90% of the JF samples remaining unclassified. Additionally, misclassifications between the JF and both the hard and soft classes occurred at a rate of 5.55% each. Notably, the PLS-DA model showed no confusion between the JF and JP classes or between the hard and soft classes (Table 2.).

In the PLS-DA model, the contribution of *LV*s to class separation was assessed using the score plots (Fig. 4). The first three *LVs* explained 73% of variations, primarily contributed to distinguishing the extreme hard and soft classes (Fig. 4a), whereas *LVs* six to 10 were mainly responsible for clustering the intermediate JP and JF classes (Fig. 4b–d).

The PLS-DA loading plots revealed wavelength regions contributing most to shell hardness classification (Fig. 5). The first two latent variables (*LV*1 and *LV*2) showed their highest absolute loadings in the 2488–2515 nm range, followed by *LV*3 and *LV*4, which were dominated by peaks between 1926 and 1948 nm. *LV*5 and *LV*6 exhibited maxima in the 1250–1474 nm region, while *LV*7 and *LV*8 placed greater emphasis on 1408–1419 nm. The final two components, *LV*9 and *LV*10, displayed prominent features between 2308 and 2423 nm, along with secondary contributions near 1910 nm.

Due to its overall higher accuracy, the PLS-DA model is selected for further analysis and applied to individual pixels of the test prawns to visualise the classification results, as shown in Fig. 6.

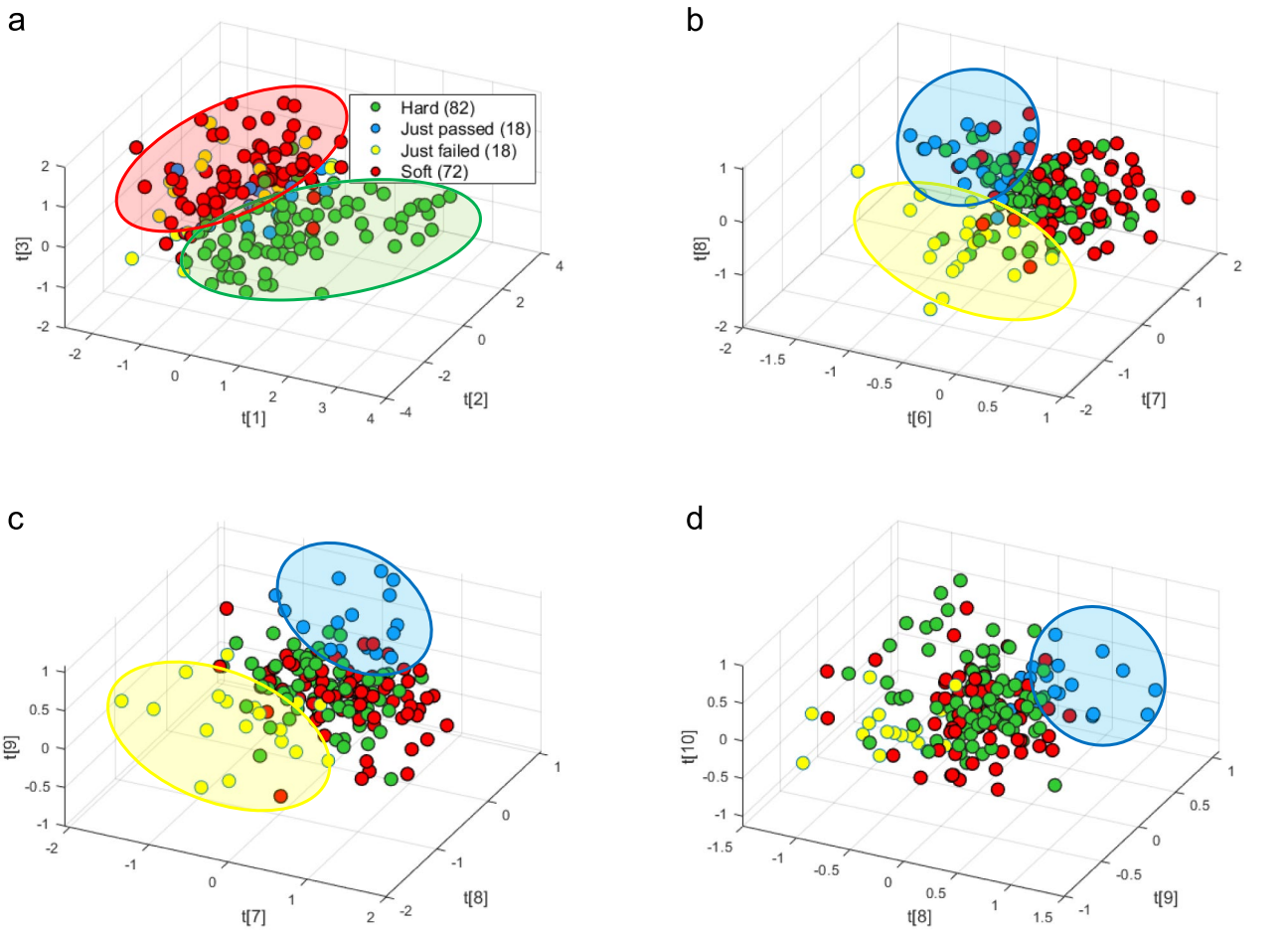

Fig. 4 Three-dimensional PLS-DA score plots illustrating prawn clustering based on transformed spectral data. Plot **a** shows the scores for latent variables (*LV*s) 1 to 3, while plots **b**, **c** and **d** display scores for *LV*s 4 to 6. The axes *t*[1] to *t*[10] represent PLS-DA scores for the respective *LV*s. Coloured circles indicate prawn texture categories: hard (green), just passed (JP, blue), just failed (JF, yellow) and soft (red). Numbers in the legend indicate the number of samples in each category. The *LV*s 1 to 10 explained 60.9%, 8.32%, 3.78%, 4.56%, 3.5%, 2%, 1%, 0.8%, 1.5% and 1.2% of the variations, respectively

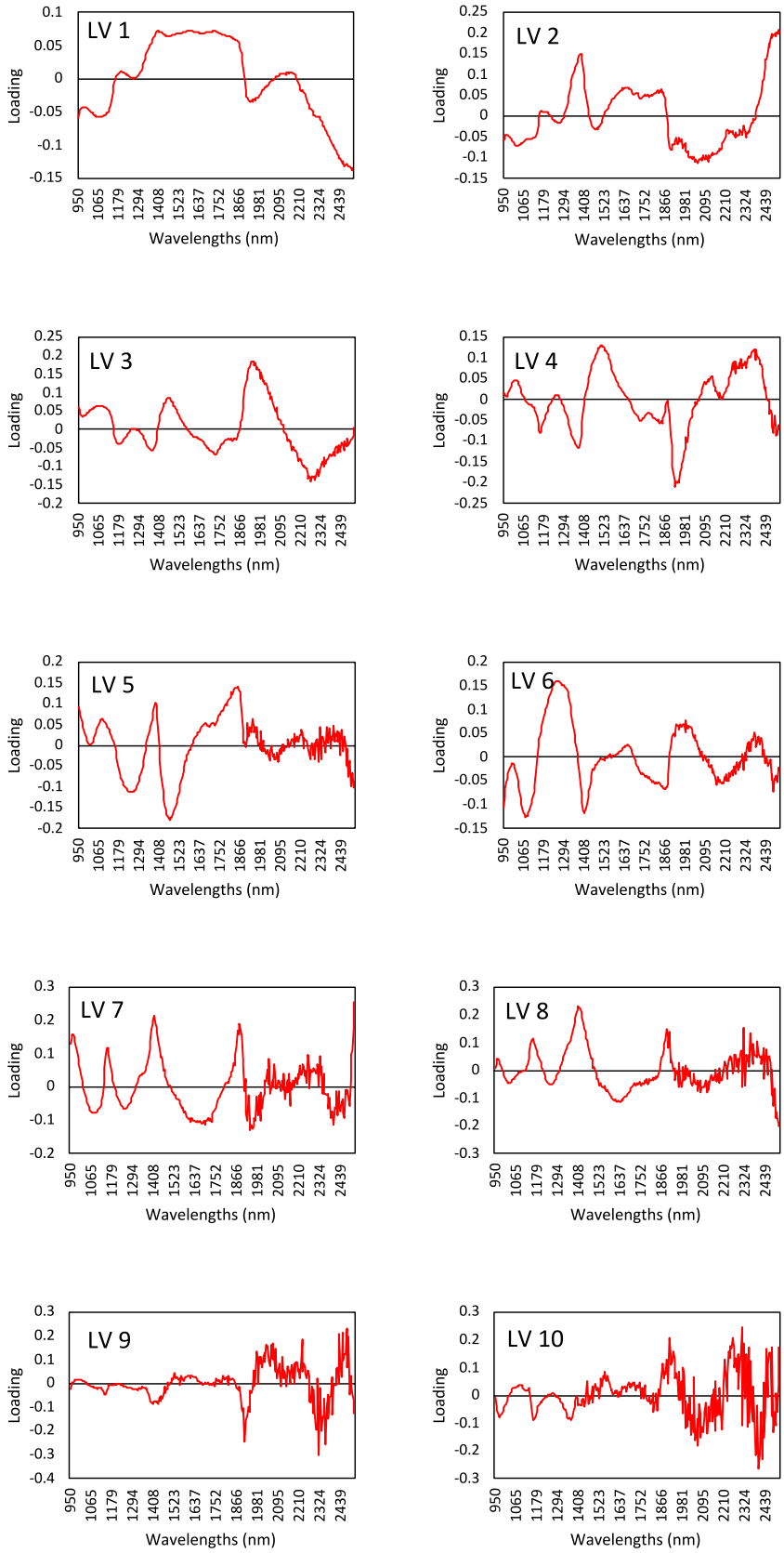

Fig. 5 PLS-DA loading plots highlighting wavelength contributions to prawn shell hardness discrimination in latent variables 1 to 10

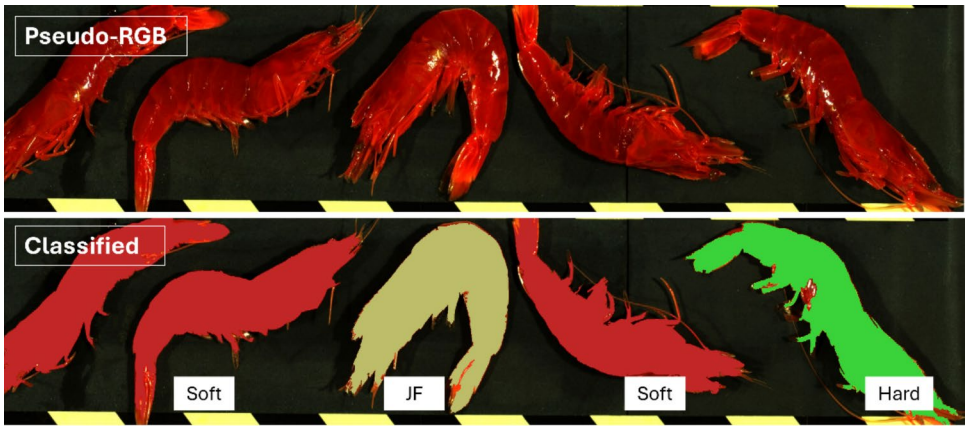

Fig. 6 Pseudo-RGB image (top), reconstructed from SWIR HSI data, and classified image (bottom) of random prawn samples from the independent test set. Colours indicate soft (red), just failed (JF, yellow) and hard (green) prawns

Discussion

Technical Aspects

The findings of this study demonstrate the potential of HSI as an objective tool for classifying prawns based on shell hardness. This aligns with our hypothesis that variations in shell properties influence the prawns' spectral signatures.

The combined interpretation of the score and loading plots indicates that the primary separation between the hard and soft classes was driven by *LV*1 to *LV*3, which assigned the greatest weight to the 2488–2515 and 1926–1948 nm regions. In contrast, differentiation of the intermediate JP and JF classes was associated with *LV*5 to *LV*10, where the dominant loadings occurred in the 1250–1474 and 2308–2423 nm ranges. These findings suggest that the hard and soft classes are mainly distinguished by reflection in the longer wavelength regions, whereas the finer separation of JP and JF relies more on variations across the shorter wavelengths.

The observed spectral differences between shell hardness classes likely arise from biochemical and structural changes in the prawn shells during hardening and mineralisation. Hard- and soft-shell prawns differ in the biochemical composition and structural properties of the shell and surrounding tissues throughout the hardening process (Baticados et al., 1986, 1987; Lemos & Weissman, 2021; Li & Cheng, 2012).

Prawn shells are primarily composed of calcium carbonate ($CaCO_3$), chitin and protein (Gbenebor et al., 2016), which contribute functional groups such as N–H, O–H, C–H and C = O (Gbenebor et al., 2016; Rollin et al., 2025). In this study, the three major spectral regions (regions 1 to 3 in Fig. 2) correspond to bond vibrations associated with stretching, bending and overtone modes of these groups (Burns & Ciurczak, 2007; Curran, 1989). The observed spectral differences between shell hardness classes may therefore reflect variations in tissue hydration, chitin content and protein deposition within the chitin matrix during post-moulting stages (Lemos & Weissman, 2021). Soft-shell prawns, immediately post-moult, tend to be more hydrated, whereas hard-shell prawns have reduced water content and more structurally organised protein (Lemos & Weissman, 2021).

Variations in the inorganic composition of prawn shells across moulting stages have also been reported. For instance, calcium and magnesium concentrations differ significantly, with soft-shell prawns exhibiting lower levels of both elements (Li & Cheng, 2012; Vijayan & Diwan, 1996). More recently, calcium and strontium were shown to increase progressively from their lowest levels immediately after moulting to peak values at the intermoult stage (Rollin et al., 2025). Structural differences have also been observed, with the cuticular layers of soft-shell prawns displaying a rough or wrinkled surface that is often disrupted and detached from the epidermis, in contrast to the more intact structure of hard-shell prawns (Baticados et al., 1987). These biochemical and structural differences across moulting stages likely underpin the ability of HSI to differentiate prawns according to shell hardness.

The SVM and PLS-DA models trained on HSI data classified prawns according to shell hardness. Both models demonstrated high accuracy on the independent test set, with PLS-DA marginally outperforming SVM. PLS-DA showed higher accuracy in classifying the extreme classes of soft- and hard-shelled prawns, whereas SVM performed better in distinguishing the intermediate class of JF, with significantly higher sensitivity. This difference likely reflects the fundamental modelling approaches; while PLS-DA projects spectral predictors onto latent variables that maximise covariance with class membership, SVM directly searches for the optimal separating hyperplane by maximising the margin between classes in the feature space. Notably, both models struggled with intermediate categories, with sensitivities falling below 90% for these classes.

Several factors may have contributed to the models' lower performance on the intermediate classes. First, the number of samples in intermediate classes was less than that in the

soft and hard categories. This may have limited the models' ability to train effectively on the intermediate classes. Data imbalance might lead to the model focussing on maximising the overall accuracy, which is mainly influenced by the majority classes and therefore the minority classes may underperform (Thabtah et al., 2020). Using imbalanced data is common, and when the number of samples permits, the larger classes can be reduced, or smaller classes can be combined to create a larger class (Davur et al., 2023; Han et al., 2021; Tahmasbian et al., 2024a, 2024b). In this study, we aimed to assess the model's performance for each class individually and identify weaknesses and, therefore, did not thin or merge any classes. Second, the initial manual classification, which serves as the reference and is currently used in Australian prawn farms, may not be entirely accurate. Differentiating between soft and hard classes is likely easier for workers, but distinguishing between intermediate classes can be more difficult and subjective. This subjectivity could have influenced the lower performance of the models for the intermediate classes. Third, the consistently lower average reflectance of the JF samples may indicate an unidentified difference other than shell hardness. While the samples were randomly scanned and individually dark and white corrected, sensor error and light variation seem unlikely to account for the issue. However, further experimentation and control of other factors, such as sample size and reference data, are needed to fully confirm this.

To address these limitations, we recommend using a larger dataset with a balanced number of samples across all shell hardness and size classes. This would improve the model's training process. Additionally, developing a quantitative method for the reference classification, as an alternative to the subjective manual method, is important. Since the quantitative reference method would only be used during calibration, slower and more accurate techniques, such as measuring shell thickness manually or chemically analysing the shells, could be considered.

Applications

This study demonstrated the potential of SWIR HSI for determining prawn shell hardness levels. The technology provides a fast, non-destructive, and accurate alternative to the current manual identification and classification process, enabling consistent and reliable prawn classification. This offers the potential for integration into automated systems for more efficient and precise sorting. The machine learning model developed using the HSI data was able to differentiate between prawns with different shell hardness levels. Given HSI's compatibility with conventional machine vision systems used for monitoring shape, size and weight (Hong et al., 2014; Pan et al., 2009; zhang et al., 2014), it offers enhanced product management and pricing by enabling classification based on varying quality levels including visual and internal characteristics.

The camera used in this study was a high-resolution 288-channel device with a maximum speed of 400 frames per second. While the full spectral range (950–2500 nm) was used in this research, future studies should focus on reducing the number of wavelengths to only the most important ones. This will increase scanning speed and reduce data size. The camera and lens also measured 384 pixels per line, covering a 10 cm width. Increasing the measurement width by adjusting the distance between the sample and the camera, using a different lens, may result in a reduction in spatial resolution. It is unclear whether this decrease in spatial resolution would affect classification accuracy. Since our models were trained using the average reflectance values for each prawn (the average of all pixels), it suggests that the technology may not be sensitive to spatial resolution.

HSI data, when analysed using the machine learning model, can serve as the core decision-making system for a sorting machine. This can be implemented in various setups, including assisted-manual systems, where HSI identifies and displays samples for removal by workers, or fully automatic systems, where HSI triggers a mechanical separation process.

Overall, this study highlights the effectiveness of HSI technology, combined with machine learning, to accurately, rapidly and non-destructively identify prawn shell hardness levels, contributing to product consistency and quality.

Conclusions

In conclusion, this study highlighted the effectiveness of SWIR hyperspectral imaging technology combined with machine learning in accurately determining prawn shell hardness levels. The developed models demonstrated high classification accuracy, particularly for extreme shell hardness classes of hard and soft, and showed potential for differentiating intermediate categories. The non-destructive, fast and reliable nature of this method provides a promising alternative to the current manual sorting process, while also offering the opportunity for future automation. With further refinement, such as the use of larger, balanced datasets and quantitative reference methods, HSI can significantly improve the consistency and efficiency of prawn sorting, benefiting both the industry and consumers by ensuring high-quality, uniform products.

Acknowledgements The authors would like to thank Dr. Kimberley Wockner, Dr. Andrew Norris and Mr. Paul Stewart (Queensland Department of Primary Industries) and Mr. Jackson Taber (Australian Prawn Farmers Association) for facilitating connections with the prawn industry.

Author Contribution I.T. secured funding, designed the experiment, provided resources, conducted laboratory work and data analysis, and interpreted the results. N.O. performed laboratory analysis. T.C. provided resources. S.H.B. provided resources and contributed to experimental design. All authors contributed to drafting and reviewing the manuscript.

Funding Open Access funding enabled and organized by CAUL and its Member Institutions. This project was funded by the Department of Primary Industries, Queensland Government, Australia (Concept 1269).

Data Availability The data is provided within the manuscript. The raw data may be available uopon request from the corresponding author.

Declarations

Competing interests The authors declare no competing interests.

References

Balaban, M. O., Yeralan, S., & Bergmann, Y. (1995). Determination of count and uniformity ratio of shrimp by machine vision. *Journal of Aquatic Food Product Technology, 3*(3), 43–58.

Baticados, M. C. L., Coloso, R. M., & Duremdez, R. C. (1986). Studies on the chronic soft-shell syndrome in the tiger prawn, *Penaeus monodon* Fabricius, from brackishwater ponds. *Aquaculture, 56*(3), 271–285.

Baticados, M., Coloso, R., & Duremdez, R. (1987). Histopathology of the chronic soft-shell syndrome in the tiger prawn *Penaeus monodon*. *Diseases of Aquatic Organisms, 3*(1), 13–28.

Burns, D. A., & Ciurczak, E. W. (2007). *Handbook of near-infrared analysis*. CRC Press.

Chicco, D., & Jurman, G. (2020). The advantages of the Matthews correlation coefficient (MCC) over F1 score and accuracy in binary classification evaluation. *Bmc Genomics*. https://doi.org/10.1186/s12864-019-6413-7

Chong, R. S.-M. (2022). Chapter 45 - Soft shell and blue shell syndrome in shrimp. In F. S. B. Kibenge, B. Baldisserotto, & R. S.-M. Chong (Eds.), *Aquaculture pathophysiology* (pp. 295–297). Academic Press.

Curran, P. J. (1989). Remote sensing of foliar chemistry. *Remote Sensing of Environment, 30*(3), 271–278.

Dai, Q., Cheng, J.-H., Sun, D.-W., & Zeng, X.-A. (2014). Potential of hyperspectral imaging for non-invasive determination of mechanical properties of prawn (*Metapenaeus ensis*). *Journal of Food Engineering, 136*, 64–72.

Davur, Y. J., Kämper, W., Khoshelham, K., Trueman, S. J., & Bai, S. H. (2023). Estimating the ripeness of Hass avocado fruit using deep learning with hyperspectral imaging. *Horticulturae, 9*(5), Article 599.

Gama, T., Farrar, M. B., Tootoonchy, M., Wallace, H. M., Trueman, S. J., Tahmasbian, I., & Hosseini Bai, S. (2024). Hyperspectral imaging predicts free fatty acid levels, peroxide values, and linoleic acid and oleic acid concentrations in tree nut kernels. *LWT - Food Science and Technology, 199*, Article Article 116068. https://doi.org/10.1016/j.lwt.2024.116068

Gbenebor, O. P., Adeosun, S. O., Lawal, G. I., & Jun, S. (2016). Role of CaCO3 in the physicochemical properties of crustacean-sourced structural polysaccharides. *Materials Chemistry and Physics, 184*, 203–209.

Han, Y., Liu, Z., Khoshelham, K., & Bai, S. H. (2021). Quality estimation of nuts using deep learning classification of hyperspectral imagery. *Computers and Electronics in Agriculture, 180*, Article Article 105868.

Hong, H., Yang, X., You, Z., & Cheng, F. (2014). Visual quality detection of aquatic products using machine vision. *Aquacultural Engineering, 63*, 62–71.

Lee, D. J., Xiong, G., Lane, R. M., & Zhang, D. (2012). An efficient shape analysis method for shrimp quality evaluation. *2012 12th International Conference on Control Automation Robotics & Vision (ICARCV)*.

Lemos, D., & Weissman, D. (2021). Moulting in the grow-out of farmed shrimp: A review. *Reviews In Aquaculture, 13*(1), 5–17. https://doi.org/10.1111/raq.12461

Li, C.-H., & Cheng, S.-Y. (2012). Variation of calcium levels in the tissues and hemolymph of *Litopenaeus vannamei* at various molting stages and salinities. *Journal of Crustacean Biology, 32*(1), 101–108.

Liu, Z. (2020). Soft-shell shrimp recognition based on an improved AlexNet for quality evaluations. *Journal of Food Engineering, 266*, Article 109698.

Liu, Z., Cheng, F., & Zhang, W. (2016). Identification of soft shell shrimp based on deep learning. 2016 ASABE Annual International Meeting. https://doi.org/10.13031/aim.20162455470

Lu, H., Song, A., Li, M., Yao, X., Cai, Y., Dong, L., Kang, D., & Liu, Y. (2025). Evaluation of the freshness (TVB-N) of pork patty during storage based on PLS-DA, SVM and BP-ANN models. *Food Control, 171*, Article 111121. https://doi.org/10.1016/j.foodcont.2024.111121

Luzuriaga, D. A., Balaban, M. O., & Yeralan, S. (1997). Analysis of visual quality attributes of white shrimp by machine vision. *Journal Of Food Science, 62*(1), 113–118.

Manley, M. (2014). Near-infrared spectroscopy and hyperspectral imaging: Non-destructive analysis of biological materials. *Chemical Society Reviews, 43*(24), 8200–8214. https://doi.org/10.1039/c4cs00062e

Menesatti, P., Costa, C., & Aguzzi, J. (2010). Chapter 8 - Quality evaluation of fish by hyperspectral imaging. In D.-W. Sun (ed.), *Hyperspectral Imaging for Food Quality Analysis and Control* (pp. 273–294). Academic Press.

Pan, P.-M., Li, J.-P., Lv, G.-L., Yang, H., Zhu, S.-M., & Lou, J.-Z. (2009). Prediction of shelled shrimp weight by machine vision. *Journal Of Zhejiang University Science B, 10*, 589–594.

Park, B., & Lu, R. (2015). *Hyperspectral imaging technology in food and agriculture*. Springer.

Qu, J.-H., Cheng, J.-H., Sun, D.-W., Pu, H., Wang, Q.-J., & Ma, J. (2015). Discrimination of shelled shrimp (*Metapenaeus ensis*) among fresh, frozen-thawed and cold-stored by hyperspectral imaging technique. *LWT - Food Science and Technology, 62*(1, Part 1), 202–209. https://doi.org/10.1016/j.lwt.2015.01.018

Rollin, M., Xuereb, B., Coulaud, R., Loisel, V., Poret, A., Duflot, A., Le Foll, F., Picard, C., & Hucher, N. (2025). The use of physicochemical properties to assess changes in the cuticle structure of crustaceans: Case of the prawn *Palaemon serratus* and its moult cycle. *Comparative Biochemistry and Physiology Part A: Molecular & Integrative Physiology, 302*, Article 111801.

Seididamyeh, M., Tahmasbian, I., Phan, A. D. T., & Sultanbawa, Y. (2024). Geographical origin discrimination of lemon myrtle (*Backhousia citriodora*) leaf powder using near-infrared hyperspectral imaging. *Food Bioscience, 59*, Article Article 103946.

Siesler, H. W., Ozaki, Y., Kawata, S., & Heise, H. M. (2008). *Near-infrared spectroscopy: Principles, instruments, applications*. John Wiley & Sons.

Siripatrawan, U., & Makino, Y. (2024). Assessment of food safety risk using machine learning-assisted hyperspectral imaging: Classification of fungal contamination levels in rice grain. *Microbial Risk Analysis, 27*, Article 100295. https://doi.org/10.1016/j.mran.2024.100295

Siripatrawan, U., & Makino, Y. (2025). Rapid and chemical-free technique based on hyperspectral imaging combined with artificial intelligence for monitoring quality and shelf life of dried shrimp. *Food Research International, 213*, Article 116422. https://doi.org/10.1016/j.foodres.2025.116422

Sun, D.-W. (2010). *Hyperspectral imaging for food quality analysis and control*. Elsevier.

Sun, D., Weng, H., He, X., Li, L., He, Y., & Cen, H. (2019). Combining near-infrared hyperspectral imaging with elemental and isotopic analysis to discriminate farm-raised Pacific white shrimp from high-salinity and low-salinity environments. *Food Chemistry, 299*, Article 125121.

Tahmasbian, I., McMillan, M. N., Kok, J., & Courtney, A. J. (2024). Underwater hyperspectral imaging technology has potential to differentiate and monitor scallop populations. *Reviews in Fish Biology and Fisheries, 34*(1), 371. https://doi.org/10.1007/s11160-023-09817-z

Tahmasbian, I., Stewart, P., Charles, T., & Hosseini Bai, S. (2024). *Real-time determination of prawn shell hardness is possible using machine learning-powered hyperspectral imaging: A pathway to automation.* PROAQUA APFA Symposium, 7 – 8 August 2024, Brisbane, Australia.

Tahmasbian, I., Wallace, H. M., Gama, T., & Hosseini Bai, S. (2021). An automated non-destructive prediction of peroxide value and free fatty acid level in mixed nut samples. *LWT - Food Science and Technology, 143*, Article 110893. https://doi.org/10.1016/j.lwt.2021.110893

Thabtah, F., Hammoud, S., Kamalov, F., & Gonsalves, A. (2020). Data imbalance in classification: Experimental evaluation. *Information Sciences, 513*, 429–441.

Vijayan, K. K., & Diwan, A. D. (1996). Fluctuations in Ca, Mg and P levels in the hemolymph, muscle, midgut gland and exoskeleton during the moult cycle of the Indian white prawn, *Penaeus indicus* (Decapoda: Penaeidae). *Comparative Biochemistry and Physiology, Part A: Physiology, 114*(1), 91–97.

Xi, Q., Chen, Q., Ahmad, W., Pan, J., Zhao, S., Xia, Y., Ouyang, Q., & Chen, Q. (2025). Quantitative analysis and visualization of chemical compositions during shrimp flesh deterioration using hyperspectral imaging: A comparative study of machine learning and deep learning models. *Food Chemistry, 481*, Article 143997. https://doi.org/10.1016/j.foodchem.2025.143997

Xu, W., Zhang, F., Wang, J., Ma, Q., Sun, J., Tang, Y., Wang, J., & Wang, W. (2022). Real-time monitoring of the quality changes in shrimp (*Penaeus vannamei*) with hyperspectral imaging technology during hot air drying. *Foods, 11*(20), Article 3179.

Ye, R., Chen, Y., Guo, Y., Duan, Q., Li, D., & Liu, C. (2020). NIR hyperspectral imaging technology combined with multivariate methods to identify shrimp freshness. *Applied Sciences, 10*(16), Article 5498.

zhang, C., Guo, C., Liu, F., Kong, W., He, Y., & Lou, B. (2016). Hyperspectral imaging analysis for ripeness evaluation of strawberry with support vector machine. *Journal of Food Engineering, 179*, 11–18.

Zhang, D., Lillywhite, K. D., Lee, D.-J., & Tippetts, B. J. (2014). Automatic shrimp shape grading using evolution constructed features. *Computers and Electronics in Agriculture, 100*, 116–122.